

Preconditioning Hamiltonian Monte Carlo by minimizing Fisher Divergence

Adrian Seyboldt* Eliot L. Carlson† Bob Carpenter‡

March 20, 2026

Although Hamiltonian Monte Carlo (HMC) scales as $O(d^{1/4})$ in dimension, there is a large constant factor determined by the curvature of the target density. This constant factor can be reduced in most cases through preconditioning, the state of the art for which uses diagonal or dense penalized maximum likelihood estimation of (co)variance based on a sample of warmup draws. These estimates converge slowly in the diagonal case and scale poorly when expanded to the dense case. We propose a more effective estimator based on minimizing the sample Fisher divergence from a linearly transformed density to a standard normal distribution. We present this estimator in three forms, (a) diagonal, (b) dense, and (c) low-rank plus diagonal. Using a collection of 114 models from `posteriorsdb`, we demonstrate that the diagonal minimizer of Fisher divergence outperforms the industry-standard variance-based diagonal estimators used by Stan and PyMC by a median factor of 1.3. The low-rank plus diagonal minimizer of the Fisher divergence outperforms Stan and PyMC’s diagonal estimators by a median factor of 4.

Keywords: Hamiltonian Monte Carlo, Fisher divergence, adaptation, preconditioning, Bayesian inference, Markov chain Monte Carlo

1. Introduction

Hamiltonian Monte Carlo (HMC) is a Markov Chain Monte Carlo (MCMC) method that is widely used in Bayesian inference for sampling from differentiable high-dimensional posterior distributions (Betancourt, 2018; Neal, 2011). By simulating Hamiltonian trajectories in a phase space consisting of a position $x \in \mathbb{R}^d$ augmented with a momentum $\rho \in \mathbb{R}^d$, HMC can explore high-dimensional parameter spaces more efficiently both in theory and in practice than gradient-free MCMC techniques such as random walk Metropolis and Gibbs sampling. HMC’s scalability makes it popular in probabilistic programming libraries based on automatic differentiation, like PyMC (Salvatier et al., 2016), Stan (Carpenter et al., 2017), NumPyro (Phan et al., 2019) and Turing.jl (Ge et al., 2018). However, HMC struggles with the stiff posteriors induced by multiscale distributions, especially when the scaling is induced by correlation rather than through independent parameters and when the eigenvectors varies by position.

1.1. Preconditioning Hamiltonian Monte Carlo

A common approach to mitigating HMC’s sensitivity to target geometry is to *precondition* the original density using a parameter transform—this is what all the probabilistic programming

*PyMC Labs, adrian.seyboldt@gmail.com

†Center for Computational Mathematics, Flatiron Institute, ecarlson@flatironinstitute.org

‡Center for Computational Mathematics, Flatiron Institute, bcarpenter@flatironinstitute.org

languages do, for example. After sampling, the preconditioned sample must be inverse transformed to recover a sample of the parameters of interest.

The most common approach to preconditioning is through a positive-definite *mass matrix* M , whereby in the leapfrog algorithm, the auxiliary momentum variables ρ are resampled from $\mathcal{N}(0, M)$ instead of the default isotropic $\mathcal{N}(0, I)$, and the momentum is transformed by M^{-1} before the position updates to match (Neal, 2011). Following Betancourt (2018), the HMC samplers of all of the probabilistic programming languages in wide use precondition with a mass matrix that targets the inverse of a regularized sample covariance estimate from warmup draws. The mass matrix is taken to be diagonal by default to avoid the high computational cost of using a dense mass matrix (cubic time to invert and factor for momentum resampling, and quadratic per leapfrog step in the Hamiltonian simulations). The diagonal approach aims to rescale the dimensions such that each has unit variance.

This is often inadequate for highly correlated target geometries or those with varying curvature. In these cases, practitioners must manually reparameterize models to achieve efficient sampling. Even where possible, this process is time-consuming and requires expertise. In most cases, the optimal reparameterization depends on the data, meaning the same model requires different parameterizations when fitted to new data. For example, depending on how informative the prior and data are, hierarchical models for varying effects, of which there are typically several in applied models, might require centered or non-centered parameterizations (Papaspiliopoulos et al., 2007; Betancourt and Girolami, 2015).

1.2. Fisher HMC

Fisher HMC, introduced here, adapts a transformation of the target distribution with the objective of minimizing the Fisher divergence from the transformed distribution to a standard normal. In this paper, we focus on affine transformations, which can be handled via a mass matrix; see Section B for a more general perspective. As well as using warmup draws as in standard adaptation, Fisher HMC uses the scores of the warmup draws (i.e., the derivatives of the target log density evaluated at the warmup draws). The scores require no additional computation because they are required for the Hamiltonian simulation step of HMC. We include specific algorithms for three classes of positive-definite mass matrices: diagonal, dense, and low rank plus diagonal.

1.3. Summary of contributions

Our primary contributions are as follows.

1. We introduce a novel mass-matrix adaptation objective—minimizing the Fisher divergence from the preconditioned target density to a standard normal.¹
2. We provide an analysis of the resulting condition numbers for multivariate normal targets.
3. We introduce an efficient scheme for estimating mass matrices using warmup draws and their scores and apply it to diagonal, dense, and low-rank plus diagonal mass matrices.
4. We experimentally demonstrate that `nutpie`'s Fisher HMC outperforms the No-U-Turn Sampler's covariance-based mass matrix estimates on a wide range of model classes.

2. Theoretical motivation for Fisher HMC

HMC is a gradient-based method, meaning that the algorithm computes the partial derivatives of the log posterior density, or *scores*. Given a target density $p(x)$, its score function is defined by

$$S(x) = \frac{\partial}{\partial x} \log p(x).$$

While these scores contain useful information about the target density, the computationally tractable preconditioning methods in wide use (Carpenter et al., 2017; Bales et al., 2019) ignore them. We discuss why and how this information can be valuable for constructing a preconditioner for HMC sampling.

¹Section B provides the geometric motivation for Fisher divergence.

2.1. An example with a normal target density

To illustrate how valuable scores are, consider a univariate normal target density $p(x) = \mathcal{N}(x \mid \mu, \sigma^2)$ for $x, \mu \in \mathbb{R}$ and $\sigma \in (0, \infty)$. The log density for a univariate normal is

$$\log p(x) \propto -\frac{1}{2} \left(\frac{x - \mu}{\sigma} \right)^2,$$

and the score function is

$$S(x) = -\frac{x - \mu}{\sigma^2}.$$

Suppose we have a pair of distinct samples, $x^{(1)}, x^{(2)} \sim \mathcal{N}(\mu, \sigma^2)$ along with their corresponding scores $\alpha^{(1)} = S(x^{(1)})$ and $\alpha^{(2)} = S(x^{(2)})$. A little algebra shows that two draws are sufficient to identify the true parameters as

$$\mu = \bar{x} + \sigma^2 \bar{\alpha} \quad \sigma^2 = \sqrt{\text{var}(x)/\text{var}(\alpha)}. \quad (1)$$

where $\bar{x}, \text{var}(x)$ and $\bar{\alpha}, \text{var}(\alpha)$ are the means and variances of the vectors $x = [x^{(1)} \ x^{(2)}]$ and $\alpha = [\alpha^{(1)} \ \alpha^{(2)}]$, respectively.²

Estimators based solely on samples from a distribution are always limited by the Cramér–Rao bound. In contrast, estimators that incorporate sample score information can bypass this bound and converge at a faster rate (e.g., the two steps shown above for the univariate normal). Later, we will see that for general multivariate distributions, an exact covariance estimate requires a number of draws equal to one plus the dimension of the distribution.

2.2. Fisher divergence

Let $p_{\mathcal{T}}(x)$ be a density on the *target space* \mathcal{T} from which we want to sample. We apply a change of variables via the diffeomorphism

$$F: \mathcal{A} \rightarrow \mathcal{T}$$

that transforms samples from an auxiliary *adapted space* \mathcal{A} onto \mathcal{T} ³. Here \mathcal{T} and \mathcal{A} denote the same ambient space \mathbb{R}^d , but we maintain distinct notation to emphasize their different roles.

By the change-of-variables formula, the induced density on \mathcal{A} is

$$p_{\mathcal{A}}(y; F) = p_{\mathcal{T}}(F(y)) |\det J_F(y)|,$$

where J_F is the Jacobian of F and $|\det J_F(y)|$ its absolute determinant. When the choice of F is clear from context, we omit it from the notation and write $p_{\mathcal{A}}(y)$ for $p_{\mathcal{A}}(y; F)$.

Given an affine transformation $F(y) = Ay + \mu$ with $(AA^T)^{-1} = M$, sampling from $p_{\mathcal{A}}$ is equivalent to sampling from $p_{\mathcal{T}}$ with mass matrix M (Neal, 2011).⁴

We would like to choose a preconditioner F^* from a rich enough family \mathcal{F} of transformations that the transformed density $p_{\mathcal{A}}$ will be close a standard normal distribution. Any measure of divergence D from $p_{\mathcal{A}}$ to $\mathcal{N}(0, I)$ can be used to define an optimal transform F^* drawn from the family \mathcal{F} of transforms,

$$F^* = \arg \min_{F \in \mathcal{F}} D[p_{\mathcal{A}}(\cdot; F) \parallel \mathcal{N}(0, I)]. \quad (2)$$

In practice, we will use a Monte Carlo estimate of the divergence based on warmup samples from the target distribution $p_{\mathcal{T}}$. This objective is reminiscent of variational inference, where one minimizes $D[\mathcal{N}(0, I) \parallel p_{\mathcal{A}}]$ (Wainwright and Jordan, 2008). Here, however, we take the divergence in the opposite direction, $D[p_{\mathcal{A}} \parallel \mathcal{N}(0, I)]$.

The most widely applied divergence is the Kullback-Leibler (KL) divergence. The KL divergence from p to q measures the cost of using density q to encode outcomes from distribution p :

$$D_{\text{KL}}[p \parallel q] = \int p(y) \log \left(\frac{p(y)}{q(y)} \right) dy.$$

²The answer is the same with variance taken to be the maximum likelihood estimate or unbiased estimate.

³Since F is a diffeomorphism, the direction of the map does not change any results. We define it from the adapted space to the target space, in line with the literature on normalizing flows.

⁴The choice of matrix square root here does not matter.

The divergence is always non-negative, equal to zero if and only if the arguments match, but it is not symmetric.

Minimizing the KL divergence leads to the choice of inverse mass matrix equal to the covariance of the draws, $M^{-1} = \text{cov}(x)$ or, if restricted to be diagonal, $M^{-1} = \text{diag}(\text{var}(x))$; see [Section C.3](#) for a proof. [Tran and Kleppe \(2024\)](#) minimized the divergence from the distribution of the scores $p_{\mathcal{T}}$ to a standard normal distribution, which results in a mass matrix estimate equal to the variance of the scores, $M = \text{var}(\alpha)$.

Minimizing KL divergence for mass matrix estimation using either scores or draws alone is suboptimal even for Gaussian targets, because it does not penalize both large and small eigenvalues of the covariance matrix equally; see [Section 2.3](#) for more details. Practically speaking, this is because it concentrates on minimizing divergence to either the score covariance or draw covariance, but does not use the information from both simultaneously. We propose using Fisher divergence instead of KL divergence. Fisher divergence uses information from both the draws and scores to condition both large and small eigenvalues. The definition of Fisher divergence is as follows; [Section B](#) contains a more general geometric definition.

Definition 2.1 (Fisher divergence). *Let p and q be two differentiable probability densities supported in \mathbb{R}^d , and let $\|v\|_{G^{-1}} = (v^T G^{-1} v)^{1/2}$ be a norm, where G is a symmetric positive definite matrix. The Fisher divergence from p to q is*

$$D_F[p \parallel q] = \int p(y) \left\| \frac{\partial}{\partial y} \log \left(\frac{q(y)}{p(y)} \right) \right\|_{G^{-1}}^2 dy.$$

Since scores transform contravariantly, we use the inverse of G in the norm.

While we don't have an inner product on our target space \mathcal{T} yet, we do have a natural norm on the adapted space $\mathcal{A} = F^{-1}(\mathcal{T})$, because the standard normal q is defined with respect to an inner product. This makes the standard Euclidean norm on the adapted space a natural choice. Suppose our target density is $p_{\mathcal{T}}(x)$. Our divergence transforms back to the original target space \mathcal{T} as

$$\begin{aligned} D_F[p_{\mathcal{A}} \parallel q] &= \int_{\mathcal{A}} p_{\mathcal{A}}(y) \left\| \frac{\partial}{\partial y} \log \left(\frac{q(y)}{p_{\mathcal{A}}(y)} \right) \right\|^2 dy \\ &= \int_{\mathcal{T}} p_{\mathcal{T}}(x) \left\| \frac{\partial}{\partial x} \log \left(\frac{q(x)}{p_{\mathcal{T}}(x)} \right) \right\|_{(J_F(F^{-1}(x)) J_F(F^{-1}(x))^T)^{-1}}^2 dx \\ &= \int_{\mathcal{T}} p_{\mathcal{T}}(x) \left\| \frac{\partial}{\partial x} \log \left(\frac{q(x)}{p_{\mathcal{T}}(x)} \right) \right\|_M^2 dx, \end{aligned}$$

where $J_F(y)$ is the Jacobian of the transformation $F: \mathcal{A} \rightarrow \mathcal{T}$.

In practice, the Fisher divergence is only estimable from a finite number of posterior draws $x^{(i)}$ and their scores, $\alpha^{(i)} = S(x^{(i)})$. With this finite sample of draws, we use the Monte Carlo estimate \widehat{D} of $D_F[p_{\mathcal{A}} \parallel \mathcal{N}(0, \mathbf{I})]$,

$$\widehat{D} = \frac{1}{N} \sum_{i=1}^N \left\| \beta^{(i)} + y^{(i)} \right\|^2,$$

where $y^{(i)}$ and $\beta^{(i)}$ are the samples and scores in the adapted space \mathcal{A} ,

$$y^{(i)} = F^{-1}(x^{(i)}) \quad \beta^{(i)} = J_F^T(y^{(i)}) \alpha^{(i)} + \frac{\partial}{\partial y} \log \left| \det J_F(y^{(i)}) \right|.$$

2.3. Condition number for Gaussian target densities

Although most of the target distributions from which we would like to sample are not strictly Gaussian, posterior distributions in Bayesian inference are often log-concave, particularly when working with large data sets, due to the Bernstein–von Mises theorem. Most of the target densities in posteriordb are log concave; those that aren't have positive-definite Hessians throughout most of their posterior probability mass ([Magnusson et al., 2025](#)). These densities are still relatively easy to analyze, so we will focus on them in this section.

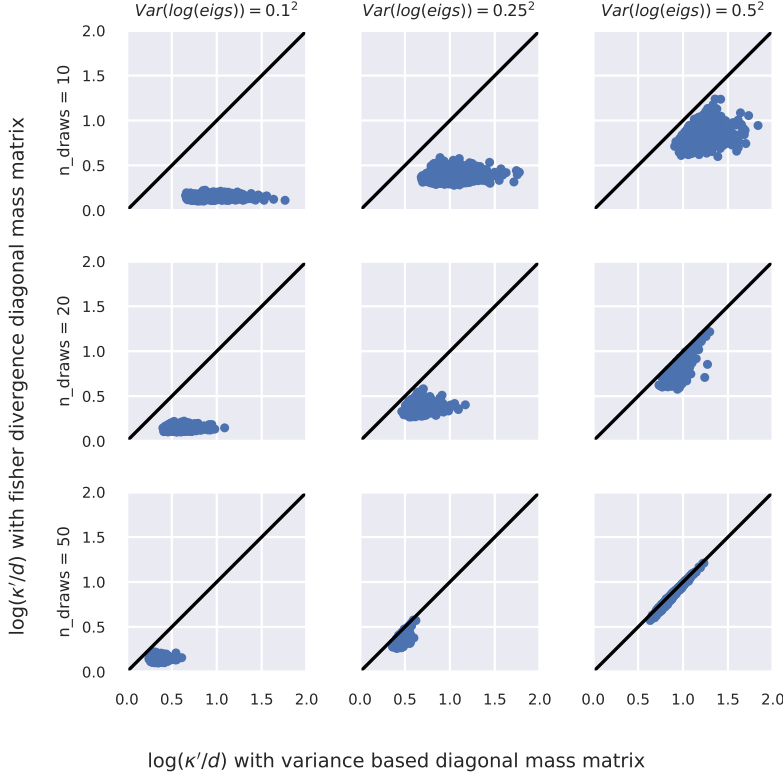


Figure 1: Simulated log condition numbers κ for Fisher- and covariance-based diagonal preconditioners. For each experiment, we generate 1000 random covariance spectra ($\Sigma = D^{1/2}U \text{diag}(\lambda^2)U^T D^{1/2}$, $U \sim \text{Uniform}((0, 200))$, $\log(\lambda_i) \sim \mathcal{N}(0, \sigma^2)$, $\log(D_{i,i}) \sim \mathcal{N}(0, 2^2)$) and simulate sets of [10, 20, 50] i.i.d. draws from $\mathcal{N}(0, \Sigma)$. We then calculate the condition number κ' of the adapted posterior with variance and Fisher-divergence based diagonal preconditioning.

HMC's efficiency is limited by the ratio of the largest to the smallest eigenvalues of the Hessian of the negative log density of the target, i.e., the condition number. Small scales constrain the step size to be small in order to remain stable, whereas large scales require many steps to complete an orbit through the target space. The leapfrog algorithm is stable only when the step size is smaller than $2/\sqrt{\max(\lambda)}$, where λ is the spectrum (i.e., the vector of eigenvalues) of the Hessian of $-\log p(x)$ evaluated at the current position x (Leimkuhler and Reich, 2004). The condition number of a matrix is defined to be the ratio of its largest to its smallest eigenvalue, $\kappa = \max(\lambda)/\min(\lambda)$. The larger the condition number, the more steps are required to complete an orbit in the largest length-scale component of the target density.

For multivariate Gaussian target densities we can be more precise about the efficiency. Suppose we have a centered multivariate Gaussian target density $\mathcal{N}(x | \mu, \Sigma)$ with eigenvalues λ for the Hessian of $-\log \mathcal{N}(x | \mu, \Sigma)$. Langmore et al. (2020) showed that the number of leapfrog steps per iteration required for efficient Hamiltonian Monte Carlo is governed by a condition-number-like quantity defined by⁵

$$\kappa' = \left(\sum_{i=1}^d \left(\frac{\max(\lambda)}{\lambda_i} \right)^2 \right)^{1/4}, \quad (3)$$

where λ is the vector of eigenvalues of the Hessian of the negative log density, $-\frac{\partial^2}{\partial x^2} \log p(x)$. In the following, we analyze how different divergence choices penalize the eigenspectrum of multivariate normal target distributions.

⁵Our definition matches that of Langmore et al. (2020), despite the difference in exponents. We use an exponent of 2 because we take the eigenvalues of $\Sigma = AA^T$, whereas they use an exponent of 4 in their definition (3.1) because they take the eigenvalues of A .

mass matrix	refresh	leapfrogs	memory	estimation
dense	$\mathcal{O}(d^3)$	$\mathcal{O}(d^2)$	$\mathcal{O}(d^2)$	$\mathcal{O}(k d^2)$
low-rank + diagonal	$\mathcal{O}(r d)$	$\mathcal{O}(r d)$	$\mathcal{O}(k d + k^2)$	$\mathcal{O}(k^3 d)$
diagonal	$\mathcal{O}(d)$	$\mathcal{O}(d)$	$\mathcal{O}(d)$	$\mathcal{O}(d)^*$

Table 1: Computational cost for three families of mass matrices in dimension d , low-rank approximation size $r \leq d$ and window size k . Refreshes are required in order to refresh momentum at the start of each HMC trajectory. The estimation cost applies only periodically during warmup, when a new mass matrix estimate is needed. The estimation cost of the diagonal case is $\mathcal{O}(d)$ amortized over the updates, a single estimation would cost $\mathcal{O}(k d)$.

Using the KL divergence on draws only conditions large eigenvalues, as can be seen from the the KL divergence from a centered multivariate Gaussian with covariance Σ to a standard Gaussian,

$$D_{\text{KL}}[\mathcal{N}(0, \Sigma) \parallel \mathcal{N}(0, \mathbf{I})] = \frac{1}{2} \sum_{i=1}^d (\lambda_i - \log(\lambda_i) - 1). \quad (4)$$

If instead we focus entirely on the scores, as [Tran and Kleppe \(2024\)](#) suggest, it conditions small eigenvalues,

$$\begin{aligned} D_{\text{KL}}[S(\mathcal{N}(0, \Sigma)) \parallel \mathcal{N}(0, \mathbf{I})] &= D_{\text{KL}}[\mathcal{N}(0, \Sigma^{-1}) \parallel \mathcal{N}(0, \mathbf{I})] \\ &= \frac{1}{2} \sum_{i=1}^d (\lambda_i^{-1} - \log(\lambda_i^{-1}) - 1). \end{aligned}$$

The Fisher divergence penalizes large and small values equally, leading to more favorable values of κ and κ' . The Fisher divergence from a centered multivariate Gaussian with spectrum λ to a standard Gaussian is

$$\begin{aligned} D_{\text{F}}[\mathcal{N}(0, \Sigma) \parallel \mathcal{N}(0, \mathbf{I})] &= \int x^\top (I - \Sigma^{-1})^2 x \mathcal{N}(x \mid 0, \Sigma) dx \\ &= \text{tr}((I - \Sigma^{-1})^2 \Sigma) \\ &= \sum_{i=1}^d (\lambda_i + \lambda_i^{-1} - 2). \end{aligned}$$

We compare simulated κ' for various Gaussian targets preconditioned with `nutpie`'s diagonal estimate and with the draws-based one in [Figure 1](#).

2.4. Affine transformations

This section presents results for three families of affine transformations, (1) diagonal, (2) diagonal plus low rank, and (3) dense. This section shows how warmup draws and their scores can be used to analytically derive the mass matrix that minimizes estimated Fisher divergence to a standard normal within the chosen family. [Table 1](#) shows the computational costs in terms of time and memory for the three approaches.

Each family can be characterized as a set of affine diffeomorphisms $F : \mathcal{A} \rightarrow \mathcal{T}$. In the most general, dense case, we have affine transforms $F_{\Sigma, \mu} : \mathbb{R}^d \rightarrow \mathbb{R}^d$, defined by

$$F_{\Sigma, \mu}(y) = A y + \mu,$$

where $\mu \in \mathbb{R}^d$ and $\Sigma \in \mathbb{R}^{d \times d}$ is symmetric and positive definite with the Cholesky factorization $\Sigma = A A^\top$. Because HMC is translation invariant, using $F_{\Sigma, \mu}$ to precondition the density is equivalent to using the mass matrix $M = \Sigma^{-1}$ ([Neal, 2011](#)). Although the location (i.e., translation) vector μ does not affect the conditioning of HMC, it can be helpful for initialization if known approximately in advance.

2.4.1. Diagonal transformations

For a diagonal transform, Σ is restricted to the diagonal form $\Sigma = \text{diag}(\sigma^2)$, where $\sigma \in (0, \infty)^d$ is a vector of strictly positive scales and σ^2 is evaluated elementwise. This yields the transform

$$F_{\text{diag}(\sigma^2), \mu}(y) = \sigma \odot y + \mu,$$

where \odot is elementwise product. Given draws $x^{(i)}$ from the target density $p_{\mathcal{T}}$ and their corresponding scores $\alpha^{(i)}$ for $i \in \{1, \dots, n\}$, the estimate of the Fisher divergence $D_{\text{F}}[p_{\mathcal{A}} \parallel q]$ is

$$\widehat{D} = \frac{1}{n} \sum_{i=1}^n \|\sigma \odot \alpha^{(i)} + \sigma^{-1} \odot (x^{(i)} - \mu)\|^2. \quad (5)$$

Theorem 2.2 (Diagonal divergence minimization). *The estimated divergence is minimized when $\mu, \sigma^2 = \mu^*, \sigma^{2*}$, where*

$$\mu^* = \bar{x} + \sigma^{2*} \odot \bar{\alpha} \quad \sigma^{2*} = \text{diag}\left(\text{diag}^{-1}(\text{cov}(x))\right) \# \left(\text{diag}\left(\text{diag}^{-1}(\text{cov}(\alpha))\right)\right)^{-1},$$

where $\text{diag}^{-1} : \mathbb{R}^{d \times d} \rightarrow \mathbb{R}^d$ extracts the diagonal of a matrix as a vector and $\#$ is the geometric mean operator in the affine-invariant Riemannian metric over symmetric, positive-definite matrices.

Proof. See Corollary A.5 for a derivation of the geometric mean operator, and Section C.6 for a proof. \square

In words, the estimated minimizer σ^* is derived by taking the geometric mean of two diagonal matrices: the diagonal of the covariance matrix of draws and the diagonal of the covariance matrix of their inverse scores. In the normal case, the estimated mean and scale recover the analytical result from the motivating example.

The geometric mean of the diagonal matrices reduces to

$$\sigma^{2*} = \sqrt{\text{diag}^{-1}(\text{cov}(x)) / \text{diag}^{-1}(\text{cov}(\alpha))},$$

where the division and square root are read elementwise; see Theorem A.5. The transformation corresponds to the inverse mass matrix

$$M^{-1} = \text{diag}(\sigma^{2*}). \quad (6)$$

The diagonal approximation is popular due to its reduced computational cost compared to dense or even low rank plus diagonal. It is the default approach used in `nutpie` and all of the widely-used HMC-based samplers. Both the mass-matrix solves required during adaptation and the mass-matrix times momentum multiplies required during the leapfrog steps are $\mathcal{O}(d)$ in time and memory; see Figure 1 for a comparison to the dense and low-rank plus diagonal families.

For adaptation during the warmup phase, mass matrix estimation requires $\mathcal{O}(nd)$ operations in d dimensions and n warmup draws. Because the solution only depends on the variances of the sequences of samples and scores, these can be calculated online in $\mathcal{O}(d)$ memory with stable arithmetic using Welford's algorithm (Welford, 1962); see Section D.1 for more details.

2.4.2. Dense transformations

The affine transform $F_{\Sigma, \mu}(y) = Ay + \mu$ for positive-definite Σ corresponds to the mass matrix $M = (AA^{\top})^{-1}$. The estimate of the Fisher divergence $D_{\text{F}}[p_{\mathcal{A}} \parallel q]$ is

$$\widehat{D} = \frac{1}{N} \sum_{i=1}^N \|A^{\top} \alpha^{(i)} + A^{-1}(x^{(i)} - \mu)\|^2. \quad (7)$$

Theorem 2.3 (Dense minimization). *The estimated Fisher divergence \widehat{D} is minimized over A when*

$$AA^{\top} \text{cov}(\alpha) A A^{\top} = \text{cov}(x). \quad (8)$$

Proof. See [Section C.1](#). □

Because $D_F[p_{\mathcal{A}} \parallel \mathcal{N}(0, \mathbf{I})]$ only depends on AA^\top and μ (see [Definition C.2](#)), A can be restricted to be symmetric positive definite without loss of generality. If the two covariance matrices are full rank, then the minimum is unique and achieved when

$$M^{-1} = \text{cov}(x) \# \text{cov}(\alpha)^{-1},$$

where $A \# B$ is the geometric mean in the affine-invariant Riemannian metric (AIRM) of symmetric, positive-definite matrices.

Theorem 2.4. *Let A be a solution to [Equation \(8\)](#) for k samples and k scores with a target distribution $\mathcal{N}(\mu, \Sigma)$. Then there is a $k - 1$ dimensional subspace of $\text{span}(x^{(i)} - \bar{x}^{(i)}) \cup \text{span}(\alpha^{(i)} - \bar{\alpha}^{(i)})$ in which Σ and the covariance of $p_{\mathcal{A}}$ match precisely.*

It follows that if $k > d + 1$, then $AA^\top = \Sigma$ and we recover the target distribution exactly.

Proof. See [Section C.4](#). □

If the number of draws k is smaller than d , [Equation \(8\)](#) has an infinite set of solutions. We add a regularization term $\gamma(\text{tr}(AA^\top) + \text{tr}((AA^\top)^{-1}))$ to our minimization objective, which yields the optimality condition

$$A A^\top (\text{cov}(\alpha) + \gamma \mathbf{I}) A A^\top = \text{cov}(x) + \gamma \mathbf{I}, \quad (9)$$

which has the unique solution

$$M_y^{-1} = (\text{cov}(x) + \gamma \mathbf{I}) \# (\text{cov}(\alpha) + \gamma \mathbf{I})^{-1}.$$

2.4.3. Low rank plus diagonal transformations

Diagonal mass matrices are inexpensive because all operations are linear in dimension, but they cannot adjust for correlation at all. Dense estimates can adjust for arbitrary correlations, but they quickly become infeasible as dimensionality increases, requiring $\mathcal{O}(d^3)$ time for estimation and $\mathcal{O}(d^2)$ per leapfrog step during Hamiltonian simulation, as well as requiring $\mathcal{O}(d^2)$ space.

In [Section C.5](#) we show that the dense solution only depends on the subspace spanned by the centered scores and gradients. Outside of this subspace, the solution to the optimization problem is unconstrained. By adding a regularization term $R(A, \mu) = \gamma(\text{tr}(AA^\top) + \text{tr}((AA^\top)^{-1}))$ to the optimization objective, we can ensure a unique solution such that AA^\top , constrained to that previously unconstrained space, is the identity matrix. We can represent and compute the resulting transformation efficiently in high dimensions as

$$F_1(y) = \left(\mathbf{I} + U \left(\text{diag}(\lambda)^{1/2} - \mathbf{I} \right) U^\top \right) y + \mu_1, \quad (10)$$

where $U \in \mathbb{R}^{d \times k}$ has orthonormal columns (i.e., $U^\top U = \mathbf{I}$). Each column of U encodes a direction and F_1 scales y in that direction by the corresponding value in $\lambda \in (0, \infty)^k$. All other orthogonal directions remain unchanged. See [Algorithm 1](#) for how to compute U and λ .

The regularization term effectively "fills up" all unidentifiable eigenvalues with ones. There is however a priori no good reason to assume that missing eigenvalues would be one. For example, if the posterior is a high-dimensional $\mathcal{N}(0, 10^{-5}\mathbf{I})$, we would use a very ill-conditioned transformation, because we are filling in eigenvalues with one instead of 10^{-5} . But we previously showed that a diagonal transformation penalizes $\sum \lambda_i + \lambda_i^{-1}$, essentially "centering" the remaining eigenvalues at one. This suggests combining the diagonal and low-rank transformations.

We split the transformation F into two parts such that $F = F_2 \circ F_1$,

$$\mathcal{A}_1 \xrightarrow{F_1} \mathcal{A}_2 \xrightarrow{F_2} \mathcal{T},$$

where F_1 is a low-rank operation and F_2 operates only on the diagonal as described in Section 2.4.1. Given a rank $k \leq d$ matrix $U \in \mathbb{R}^{d \times k}$ with orthonormal columns (i.e., $U^\top U = \mathbf{I}$),

$$F_1(y) = \left(\mathbf{I} + U \left(\text{diag}(\lambda)^{1/2} - \mathbf{I} \right) U^\top \right) y + \mu_1 \quad (11)$$

$$F_2(v) = \sigma \odot v + \mu_2. \quad (12)$$

The combined transformation $F = F_2 \circ F_1$ corresponds to the mass matrix

$$M = \text{diag}(\sigma)^{-1} \left(\mathbf{I} + U \left(\text{diag}(\lambda)^{-1} - \mathbf{I} \right) U^\top \right) \text{diag}(\sigma)^{-1}.$$

In practice, we avoid storing M and work with σ , λ and U directly, which requires only $\mathcal{O}(kd)$ storage. During sampling, we only need products $M^{-1}\rho$ and evaluations of $F(y)$ to sample from $\mathcal{N}(0, M)$, both of which can easily be achieved in $\mathcal{O}(kd)$ as well.

To further reduce the computational cost of leapfrog steps, we can omit entries in σ that are close to one and don't affect the quality of the mass matrix much anyway.

Algorithm 1 LOW-RANK-ADAPT

Require: $x \in \mathbb{R}^{d \times n}$: draws, $\alpha \in \mathbb{R}^{d \times n}$: scores, c : cutoff, γ : regularizer

for i in $0 : d - 1$ **do**

$\sigma_i \leftarrow \sqrt{\text{var}(x_i) / \text{var}(\alpha_i)}$ ▷ set coordinate-wise standard deviations

end for

$x \leftarrow (x - \bar{x}) \odot \sigma$, $\alpha \leftarrow (\alpha - \bar{\alpha}) \odot \sigma$ ▷ apply diagonal transform

$U^x \leftarrow \text{SVD}(x)$, $U^\alpha \leftarrow \text{SVD}(\alpha)$

$Q, _ \leftarrow \text{QR-THIN}([U^x \ U^\alpha])$ ▷ get jointly-spanned orthonormal basis

$P^x \leftarrow Q^\top x$, $P^\alpha \leftarrow Q^\top \alpha$ ▷ project onto shared subspace

$C^x \leftarrow P^x (P^x)^\top + \gamma I$, $C^\alpha \leftarrow P^\alpha (P^\alpha)^\top + \gamma I$ ▷ empirical covariance, regularize

$\Sigma \leftarrow \text{SPDM}(C^x, C^\alpha)$ ▷ solve $\Sigma C^\alpha \Sigma = C^x$ for Σ

$U, \Lambda \leftarrow \text{EIGENDECOMPOSE}(\Sigma)$ ▷ extract eigendecomposition

$U_c \leftarrow \{U_i : \lambda_i \leq 1/c \text{ or } \lambda_i \geq c\}$ ▷ filter eigenpairs

$\Lambda_c \leftarrow \{\lambda_i : \lambda_i \leq 1/c \text{ or } \lambda_i \geq c\}$

return Q, U_c, Λ_c

3. Adaptation schedule

In order to turn our optimal update rules into a mass-matrix adaptation algorithm, we need to introduce a schedule dictating how often during sampling the mass matrix is updated and which set of draws and scores are used for the update. While we follow roughly the standard pattern of adaptation, this section introduces two novel modifications to the algorithm used by Stan and other probabilistic programming languages.

Whether adapting a mass matrix using the posterior variance, as Stan does, or using a matrix based on the Fisher divergence, preconditioning invariably faces the same chicken-and-egg problem, namely that generating suitable posterior draws requires a good mass matrix, but estimating a good mass matrix requires acceptable posterior draws.

Algorithm 2 SYMMETRIC POSITIVE-DEFINITE MEAN (SPDM)

Require: $A, B \in \mathbb{R}^{n \times n}$ symmetric, positive-definite

$$U_A, \Lambda_A \leftarrow \text{EIGENDECOMPOSE}(A)$$

$$A^{1/2} \leftarrow U_A \text{diag}(\Lambda_A^{1/2}) U_A^\top$$

$$A^{-1/2} \leftarrow U_A \text{diag}(\Lambda_A^{-1/2}) U_A^\top$$

$$M \leftarrow A^{1/2} B A^{1/2}$$

$$U_M, \Lambda_M \leftarrow \text{EIGENDECOMPOSE}(M)$$

$$M^{1/2} \leftarrow U_M \text{diag}(\Lambda_M^{1/2}) U_M^\top$$

$$\text{return } A^{-1/2} M^{1/2} A^{-1/2}$$

Stan and other probabilistic programming languages begin with the identity transformation, collect a number of draws, then based on those draws, estimate a better transformation, and repeat (Betancourt, 2018; Phan et al., 2019; Cabezas et al., 2024). These systems, as well as `nutpie`, do not use standard HMC, but rather use the No-U-Turn Sampler (NUTS) (Hoffman and Gelman, 2014; Betancourt, 2018), where the length of the Hamiltonian trajectory is chosen dynamically.

With NUTS, it is extremely costly to generate draws with a poorly tuned mass matrix, because in ill-conditioned cases, the algorithm will require a minuscule step size for stability and a huge number of steps before satisfying the U-turn condition. This problem is exacerbated by Stan’s default cap of the number of leapfrog steps per draw of $2^{10} = 1024$. This is another way of saying that HMC is highly sensitive to condition number (Langmore et al., 2020). By default, Stan starts adaptation with a step-size adaptation window of 75 draws, using an identity mass matrix. This is followed by a mass matrix adaptation window consisting of a series of discrete intervals of increasing length, the first of which is 25 draws long. These initial 100 draws before the first adapted mass matrix can, perhaps counterintuitively, constitute a sizable fraction of the total sampling time over Stan’s default 2000 iterations.

Avoiding these costly warmup scenarios motivates the use of all available information about the posterior as quickly as possible during sampling. To this end, the `nutpie` sampler implements a faster-paced adaptation schedule than the NUTS algorithm. We propose two fairly small modifications that provide a substantial boost in efficiency.

3.1. Improved initialization

The first modification introduced by `nutpie` is that the mass matrix M is initialized to $\text{diag}(|\alpha^{(0)}|)$, where $\alpha^{(0)}$ is the score of the first draw. The absolute score is the solution to Equation (8) when $\text{cov}(\alpha)$ is taken to be the initial score squared (i.e., estimated covariance, assuming a mean of zero), and $\text{cov}(x)$ is taken to be the identity. This can also be viewed as a regularized diagonal of the gradient outer-product, which is a common approximation to the Hessian at x_0 , used in systems such as L-BFGS optimization (Nocedal and Wright, 2006). As a result, we have the following straightforward result.

Lemma 3.1 (Scale free). *The `nutpie` adaptation algorithm is scale free in the sense that sampling from the unnormalized densities $p(\theta)$ and $q(\theta) = p(c \odot \theta)$ for any vector c has the same efficiency.*

Proof. The initialization at $M = \text{diag}(|\alpha^{(0)}|)$ scales with c , as do all subsequent scores and hence trajectories. \square

3.2. More frequent updates

The second modification introduced by `nutpie` is to update the mass matrix estimates more frequently, starting from the very first draw. Stan waits until after 75 warmup iterations (by default) before it uses draws for estimating the mass matrix, in the hope that the Markov chain will

have approximately converged to the stationary distribution; this is not unreasonable, as HMC mixes very quickly. We do not want to wait that long. We would rather integrate information from draws into estimates of the mass matrix immediately upon sampling them, while also discounting very early draws as sampling progresses. We discount earlier draws because they will not be drawn from the (approximate) stationary distribution.

For diagonal mass matrix estimates, we use Welford’s algorithm to store online estimates of the variance of draws and scores to compute an up-to-date value for Equation (6) at each iteration. Instead of modifying the algorithm with a weighting scheme to taper the influence of these early draws, we periodically chop off the tail end from the set of draws our estimator is built upon. In other words, old draws are periodically wiped from the memory of the online estimate. The frequency with which this memory wipe occurs is a tunable parameter, L . With this approach, the number of draws informing the estimates after the first L oscillates between L and $2L$. The matrix used to sample draw n is always based on an estimate constructed from the sequence of draws $\theta^{(a_n)}, \dots, \theta^{(n-1)}$, where

$$a_n = \max(0, L (\lfloor n/L \rfloor - 1)).$$

The implementation of this scheme for diagonal `nutpie` is illustrated with an example of the first 20 draws in Section D.2.

Low-rank plus diagonal adaptation requires us to store the draws and the scores in the window used for estimating the mass matrix. In this case, the mass matrix is only updated at multiples of L iterations.

3.3. Step-size adaptation phases

The matrix adaptation occurs in conjunction with the dual averaging step-size adaptation of standard NUTS, which aims to tune ϵ to achieve a target acceptance rate over states in the last half of the Hamiltonian trajectories. The stochastic gradient update on which dual averaging is based assumes a squared error, so gradient descent pushes step size lower if the acceptance rate is too low and higher if it is too high, lowering the learning rate over time.

We organize warmup into three phases based on the hyperparameters used to tune the mass matrix M and step size ϵ adaptation.

1. The first 30% of warmup iterations, adapts a mass matrix with an update frequency $L = 10$ using the Metropolis acceptance probability $\exp(\min(0, \Delta H))$ where ΔH is the change in the Hamiltonian induced by the error in the leapfrog integrator.
2. The next 55% of warmup iterations use $L = 80$ and the same acceptance probability for tuning. At the start of the second phase, the step size is reinitialized in the same manner as at the first draw.
3. Following NUTS as implemented in Stan, the final 15% of the warmup draws are devoted exclusively to fine-tuning the step size ϵ . Unlike the first two phases, the third phase uses the symmetric acceptance statistic

$$\frac{2 \exp(\min(0, \Delta H))}{1 + \exp(\Delta H)}.$$

4. Implementation and evaluation on `posteriodb`

We systematically test `nutpie`’s diagonal and low-rank samplers on the models in `posteriodb`, using Stan’s default NUTS implementation as a benchmark. We run 4 chains of each sampler for 1000 warmup iterations and 1000 posterior draws on all models, using a target acceptance rate of 0.8. For `nutpie`’s low-rank mode, we use an eigenvalue cutoff $c = 2$, and regularization parameter $\gamma = 10^{-5}$. From our tests we exclude some exceptionally slow models, listed in Section E. We also discard models which did not converge for any of the solver configurations, defining convergence as if there are no divergences during the run, and the effective sample size exceeds 200 for all parameters. 114 models remained after this filtering. Among these, `nutpie`’s diagonal mode required a median $\sim 0.75x$ the number of gradient evaluations as Stan

for an effective sample. In wall time, this translated to a $\sim 1.3x$ median speedup. The low-rank mode had a median $\sim 4x$ speedup in both effective sample size per gradient evaluation and ESS per second. Detailed results can be seen in Figure 2. Additional diagnostic comparisons can be found in Section E.

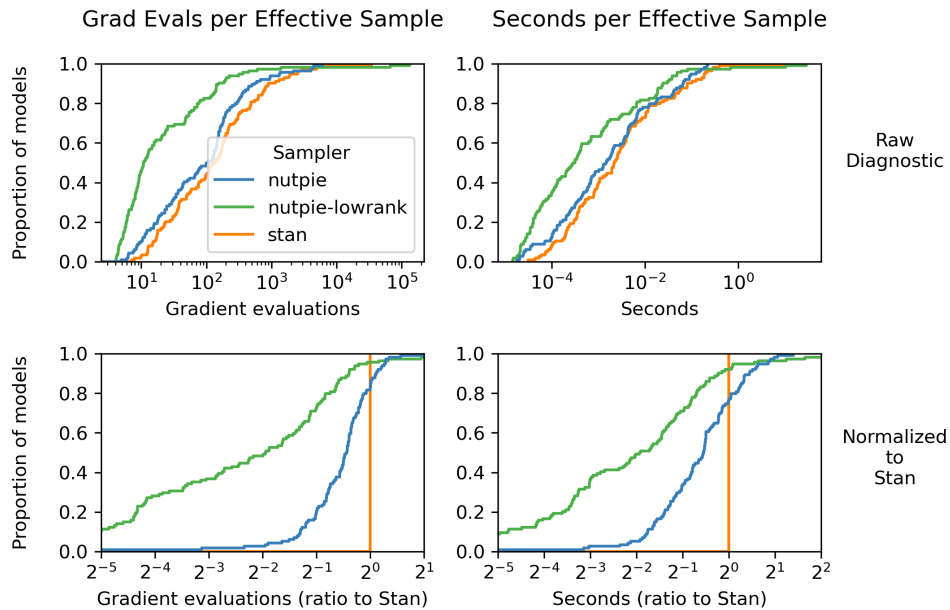


Figure 2: Cumulative distribution plots for target densities in `posteriordb`. Each line represents a different sampler, `nutpie` (blue), `Stan` (orange), and `nutpie low-rank` (green) run for 1000 warmup iterations and 1000 posterior draws. The top row of plots show the raw diagnostic, while the bottom show the ratio of the diagnostic to Stan’s. For instance, a point (x, y) on the lower gradients plot says that a fraction y of `posteriordb` models had x or fewer times the number of gradient evaluations per effective sample as Stan’s. Lines to the right of 1 show a small fraction of models for which Stan’s default outperforms the other options.

5. More general transforms

While in this paper we focus on affine transformations F , corresponding to a constant mass matrix in the HMC metric interpretation, the same framework applies to more general, nonlinear transformations that induce position-dependent metrics. This recovers a form of Riemannian HMC, where the metric is learned by minimizing the Fisher divergence. We have implemented an experimental version of this in `nutpie` that uses normalizing flows; see Section B for the geometric formulation.

6. Open-source implementation

All evaluations of Fisher-divergence based preconditioning in this paper were carried out using `nutpie`, an optimized Rust-based implementation that is distributed with a permissive open-source MIT License through the PyMC project.⁶ `Stan` was used for the NUTS comparison.⁷

7. Conclusion

We have presented algorithms to construct three novel forms of linear preconditioner for Hamiltonian Monte Carlo which incorporate information from the scores of warmup draws to

⁶See <https://pymc-devs.github.io/nutpie/>.

⁷See <https://mc-stan.org/docs/reference-manual/mcmc.html>.

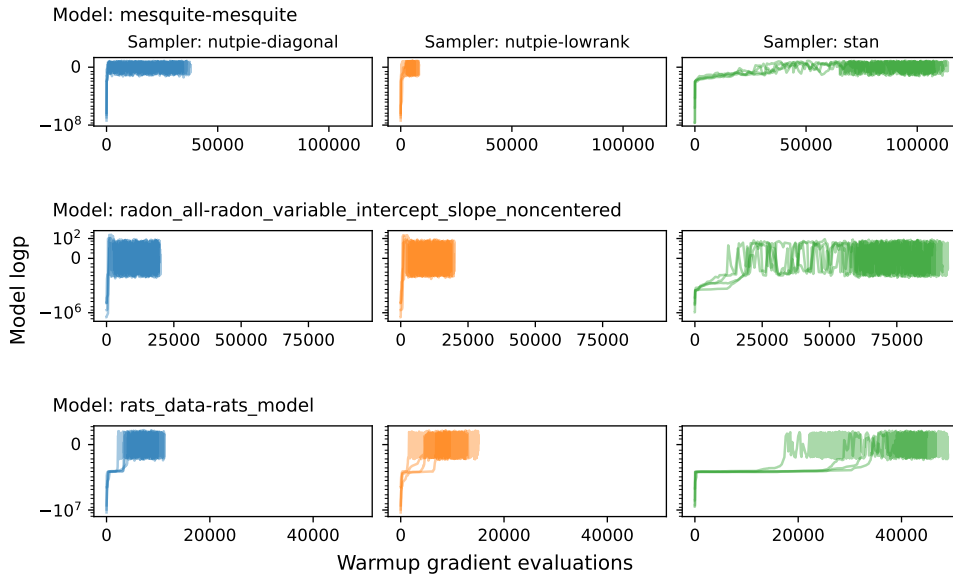


Figure 3: Trace-plot of sample log density scaled by number of gradient evaluations for three models from `posteriordb`. Each row corresponds to one model, the rows show `nutpie` with diagonal mass matrix adaptation, `nutpie` with low rank adaptation and `Stan`, respectively. The x-axis shows the number of gradient evaluations rather than the number of draws as typical with a trace-plot. All samplers run 1000 warmup draws. `nutpie` uses significantly fewer gradient evaluations in total, and avoids a long inefficient phase seen in `Stan`. Figure 7 shows this trace-plot for 15 randomly selected models from `posteriordb`.

better approximate target covariance. The added information in the scores allows for quicker adaptation of the mass matrix than state of the art HMC samplers.

We have limited our discussion to linear transformations, but the Fisher divergence framework naturally generalizes to nonlinear transformations and to transformations on Riemannian Manifolds, yielding position-dependent metrics and a practical link to Riemannian HMC. Experiments with normalizing flows parameterized by neural networks, as well as smaller model-informed transformations, are promising, and we plan to report them separately.

References

- Ando, T., Li, C.-K., and Mathias, R. (2004). Geometric means. *Linear Algebra and its Applications*, 385:305–334.
- Bales, B., Pourzanjani, A., Vehtari, A., and Petzold, L. (2019). Selecting the metric in Hamiltonian Monte Carlo. *arXiv preprint arXiv:1905.11916*.
- Betancourt, M. (2018). A conceptual introduction to Hamiltonian Monte Carlo.
- Betancourt, M. and Girolami, M. (2015). Hamiltonian Monte Carlo for hierarchical models. *Current Trends in Bayesian Methodology with Applications*, 79(30):2–4.
- Cabezas, A., Corenflos, A., Lao, J., Louf, R., Carnec, A., Chaudhari, K., Cohn-Gordon, R., Coullon, J., Deng, W., Duffield, S., et al. (2024). BlackJAX: Composable Bayesian inference in JAX. *arXiv preprint arXiv:2402.10797*.
- Carpenter, B., Gelman, A., Hoffman, M. D., Lee, D., Goodrich, B., Betancourt, M., and Riddell, A. (2017). Stan: A probabilistic programming language. *Journal of Statistical Software*, 76(1):1–32.
- Ge, H., Xu, K., and Ghahramani, Z. (2018). Turing: a language for flexible probabilistic inference. In *International Conference on Artificial Intelligence and Statistics*, pages 1682–1690. PMLR.
- Hoffman, M. D. and Gelman, A. (2014). The No-U-Turn sampler: adaptively setting path lengths in Hamiltonian Monte Carlo. *Journal of Machine Learning Research*, 15(1):1593–1623.
- Langmore, I., Dikovsky, M., Geraedts, S., Norgaard, P., and Von Behren, R. (2020). A condition number for Hamiltonian Monte Carlo. *arXiv preprint arXiv:1905.09813*.
- Leimkuhler, B. and Reich, S. (2004). *Simulating Hamiltonian Dynamics*. Cambridge University Press.
- Magnusson, M., Torgander, J., Bürkner, P.-C., Zhang, L., Carpenter, B., and Vehtari, A. (2025). posteriordb: Testing, benchmarking and developing Bayesian inference algorithms.
- Malagò, L. and Pistone, G. (2015). Information geometry of the Gaussian distribution in view of stochastic optimization. In *Proceedings of the 2015 ACM Conference on Foundations of Genetic Algorithms XIII*, pages 150–162.
- Neal, R. M. (2011). MCMC using Hamiltonian dynamics. In Brooks, S., Gelman, A., Jones, G., and Meng, X.-L., editors, *Handbook of Markov chain Monte Carlo*, pages 47–95. Chapman and Hall/CRC.
- Nocedal, J. and Wright, S. J. (2006). *Numerical Optimization*. Springer.
- Papaspiliopoulos, O., Roberts, G. O., and Sköld, M. (2007). A general framework for the parametrization of hierarchical models. *Statistical Science*, pages 59–73.
- Phan, D., Pradhan, N., and Jankowiak, M. (2019). Composable effects for flexible and accelerated probabilistic programming in NumPyro. *arXiv preprint arXiv:1912.11554*.
- Salvatier, J., Wiecki, T. V., and Fonnesbeck, C. (2016). Probabilistic programming in Python using PyMC3. *PeerJ Computer Science*, 2:e55.
- Tran, J. H. and Kleppe, T. S. (2024). Tuning diagonal scale matrices for HMC. *Statistics and Computing*, 34(6):196.
- Wainwright, M. J. and Jordan, M. I. (2008). Graphical models, exponential families, and variational inference. *Foundations and Trends in Machine Learning*, 1(1–2):1–305.
- Welford, B. (1962). Note on a method for calculating corrected sums of squares and products. *Technometrics*, 4(3):419–420.

A. The geometry of symmetric, positive-definite matrices

Our mass matrices need to be symmetric and positive definite in order to define a proper covariance over momentum vectors. Therefore, we will be working in the smooth manifold of $d \times d$ symmetric positive-definite matrices, which is conventionally denoted by \mathcal{S}_{++}^d .

A.1. The affine-invariant Riemannian metric

There is more than one metric $d(A, B)$ that can be defined over symmetric, positive-definite matrices $A, B \in \mathcal{S}_{++}^d$. We will concentrate on the affine-invariant Riemannian metric (AIRM), which is defined as follows.

Definition A.1 (AIRM). *The affine-invariant Riemannian metric on \mathcal{S}_{++}^d is defined for $P \in \mathcal{S}_{++}^d$ and tangent vectors $U, V \in T_P \mathcal{S}_{++}^d \cong \mathbb{S}^d$ by the inner product on the tangent space at P ,*

$$\langle U, V \rangle_P = \text{tr}(P^{-1}U P^{-1}V).$$

Theorem A.2 (Distance). *Distance in the affine-invariant Riemannian metric satisfies*

$$d(A, B) = \left\| \log\left(A^{-1/2} B A^{-1/2}\right) \right\|_F,$$

where the norm $\|X\|_F = \sqrt{\text{tr}(X^\top X)}$ is the Frobenius norm and the logarithm is the matrix logarithm.

Corollary A.3 (Affine invariance). *This distance function is affine-invariant in the sense that for any conforming invertible matrix X ,*

$$d(A, B) = d(X^\top A X, X^\top B X).$$

Theorem A.4 (Dense geometric mean). *Given $A, B \in \mathcal{S}_{++}^d$, their geometric mean with respect to the affine-invariant Riemannian metric is the midpoint of the unique geodesic from A to B , which is given by*

$$A \# B = A^{1/2} \left(A^{-1/2} B A^{-1/2} \right)^{1/2} A^{1/2}.$$

Proof. See [Ando et al. \(2004\)](#). □

Corollary A.5 (Diagonal geometric mean). *Given $a, b \in (0, \infty)^d$, let $A = \text{diag}(a)$ and $B = \text{diag}(b)$. The geometric mean for diagonal matrices is*

$$\text{diag}(a) \# \text{diag}(b) = \text{diag}\left(\sqrt{a \odot b}\right),$$

where \odot is elementwise multiplication and square root applies elementwise.

Proof. Diagonal multiplication, square root, and inverse square root apply elementwise to diagonal elements. □

Given a data generating density $p(x | \theta)$ with support over $x \in \mathbb{R}^d$ and parameters θ , the Fisher information metric is defined at a fixed parameter value θ by

$$I(\theta) = - \int_{\mathbb{R}^d} p(x | \theta) \frac{\partial^2}{\partial \theta \partial \theta^\top} \log p(x | \theta) dx.$$

Theorem A.6 (AIRM & Fisher info. for Gaussians). *The affine-invariant Riemannian metric is equal to the Fisher information metric for the family of centered multivariate Gaussian distributions $\mathcal{N}(0, \Sigma)$.*

Proof. See Equation (23) of [Malagò and Pistone \(2015\)](#). □

B. A geometric view of Fisher HMC

This appendix presents a coordinate-free formulation of preconditioning for HMC, extending the usual Euclidean treatment to general smooth manifolds and to nonlinear (non-affine) transformations. Such a formulation also naturally encompasses settings where the target or latent space has non-Euclidean geometry (for example, distributions on spheres, Stiefel manifolds, or other Riemannian manifolds), although we focus on the Euclidean case in the main text.

Let the *target space* be a smooth orientable manifold \mathcal{T} endowed with a posterior volume form p (the target distribution viewed as an n -form with $\int p = 1$).

We augment \mathcal{T} with a corresponding manifold of momenta to the cotangent bundle $T^*\mathcal{T}$. Any Riemannian metric g on \mathcal{T} with volume form vol_g allows us to define the Hamiltonian on the cotangent bundle $T^*\mathcal{T}$ of positions and momenta as

$$H_{g,p}(x, \rho) = \frac{1}{2} \|\rho\|_{g^{-1}(x)}^2 - \log\left(\frac{p}{\text{vol}_g}\right)(x),$$

where $p/\text{vol}_g \in \Omega^0(\mathcal{T})$ is the density of p with respect to vol_g .

Identify $T_{(x,\rho)}(T^*\mathcal{T}) \cong T_x\mathcal{T} \oplus T_x^*\mathcal{T}$. Then the Hamiltonian vector field X_H has components

$$X_H(x, \rho) = (d_\rho H_{g,p}(x, \rho), -d_x H_{g,p}(x, \rho)).$$

Alternatively, X_H is the vector field that satisfies $\iota_{X_H}\omega = dH$, where ω is the canonical symplectic form on $T^*\mathcal{T}$.

The vector field X_H induces the flow Φ_H^t and yields the following (exact) HMC algorithm: starting at position $x_0 \in \mathcal{T}$, sample momentum $\rho_0 \in T_{x_0}^*\mathcal{T} \sim \mathcal{N}(0, g_{x_0})$. Evolve the system to time t to obtain $(x_1, \rho_1) = \Phi_H^t(x_0, \rho_0)$, and return the new position x_1 .

The performance of the sampler critically depends on the choice of metric g . Suppose that we already know that a distribution q (viewed again as a volume form) on another manifold \mathcal{A} , diffeomorphic to \mathcal{T} , can be sampled efficiently with a metric μ using the Hamiltonian $H_{\mu,q}$. In practice, this is often $\mathcal{A} = \mathbb{R}^n$ with μ the constant identity metric and q the standard normal volume form.

A diffeomorphism $f: \mathcal{A} \rightarrow \mathcal{T}$ pushes the metric forward to \mathcal{T} through $f_*\mu$. This allows us to sample from p using the Hamiltonian $H_{f_*\mu,p}$ on \mathcal{T} , or equivalently, H_{μ,f^*p} on \mathcal{A} .

Since $H_{\mu,q}$ generates an efficient flow through the vector field $X_{H_{\mu,q}}$, we would like to choose f so that the vector fields $X_{H_{\mu,q}}$ and $X_{H_{\mu,f^*p}}$ are similar.

Minimizing the squared error between the two Hamiltonian vector fields on $T^*\mathcal{A}$ (evaluated at $\rho = 0$) leads to the optimization problem

$$\hat{f} = \arg \min_{f \text{ diffeo}} \int_{\mathcal{A}} \left\| X_{H_{\mu,q}}(x, 0) - X_{H_{\mu,f^*p}}(x, 0) \right\|_{\mu}^2 f^*p.$$

To evaluate this, note that the Hamiltonian vector field has components $X_H(x, \rho) = (d_\rho H, -d_x H)$. For $H_{\mu,\omega}(x, \rho) = \frac{1}{2} \|\rho\|_{\mu^{-1}}^2 - \log(\omega/\text{vol}_\mu)(x)$, we have $d_\rho H_{\mu,\omega} = \mu^{-1}\rho$ and $d_x H_{\mu,\omega} = -d \log(\omega/\text{vol}_\mu)$. Thus, the position component of the vector field is $\mu^{-1}\rho$ for both Hamiltonians (independent of the target distribution), while the momentum components differ:

$$X_{H_{\mu,q}} = \left(\mu^{-1}\rho, d \log\left(\frac{q}{\text{vol}_\mu}\right) \right), \quad X_{H_{\mu,f^*p}} = \left(\mu^{-1}\rho, d \log\left(\frac{f^*p}{\text{vol}_\mu}\right) \right).$$

The difference lies entirely in the momentum component. Moreover, it is independent of ρ , so although the choice to evaluate the squared error at $\rho = 0$ may initially seem ad hoc, the resulting objective is unchanged. Computing the squared norm with respect to μ (where the position part uses μ and the momentum part uses μ^{-1}):

$$\|X_{H_{\mu,q}} - X_{H_{\mu,f^*p}}\|_{\mu}^2 = \|0\|_{\mu}^2 + \|d \log(q/f^*p)\|_{\mu^{-1}}^2 = \|d \log(f^*p/q)\|_{\mu^{-1}}^2.$$

Therefore,

$$\hat{f} = \arg \min_{f \text{ diffeo}} \int \left\| d \log\left(\frac{f^*p}{q}\right) \right\|_{\mu^{-1}}^2 f^*p,$$

where $\|\cdot\|_{\mu^{-1}}$ denotes the norm on 1-forms induced by μ .

The resulting cost function is exactly the Fisher divergence from f^*p to q :

Definition B.1 (Fisher Divergence). *Let X be a manifold with metric g and volume forms ω_1, ω_2 that are mutually absolutely continuous. The Fisher divergence from ω_1 to ω_2 is*

$$\mathcal{F}_g(\omega_1, \omega_2) = \int_X \left\| d \log \left(\frac{\omega_1}{\omega_2} \right) \right\|_{g^{-1}}^2 \omega_1.$$

B.1. Leapfrog steps

In practice, we usually cannot compute Φ_H^t directly. But if the Hamiltonian can be written as the sum of two functions $H = V + K$ such that Φ_V^t and Φ_K^t can be computed efficiently, we can use the leapfrog integrator to approximate

$$\Phi_H^\epsilon \approx \Phi_V^{\epsilon/2} \circ \Phi_K^\epsilon \circ \Phi_V^{\epsilon/2}.$$

Different splits of H are possible, but generally we choose $K = \langle \rho, \rho \rangle_{g^{-1}}/2$ and $V = -\log\left(\frac{p}{\text{vol}_g}\right)$, such that Φ_K^t is the exponential map with respect to g , and V depends only on x and not on ρ , so that Φ_V^t is also easy to compute⁸. Algorithm 3 shows how we can use this to compute approximate Φ_H^t in a reversible manner.

Algorithm 3 TRANSFORMED-LEAPFROG

Require: x : draw, v : velocity, L : num. steps, ϵ : step size, f : diffeomorphism

$x^{(0)} \leftarrow x, \quad v^{(0)} \leftarrow v$

$y \leftarrow f^{-1}(x^{(0)})$

$\delta \leftarrow \frac{\partial}{\partial y} \log\left(\frac{f^* p}{\lambda_{\mathcal{A}}}\right)(y)$ ▷ evaluate score on \mathcal{A}

for $i = 1$ **to** L **do**

$v^{(i+1/2)} \leftarrow v^{(i)} - \frac{\epsilon}{2} \delta$ ▷ half-step velocity

$y \leftarrow y + \epsilon v^{(i+1/2)}$ ▷ full-step position (mass matrix = I)

$\delta \leftarrow \frac{\partial}{\partial y} \log\left(\frac{f^* p}{\lambda_{\mathcal{A}}}\right)(y)$

$v^{(i+1)} \leftarrow v^{(i+1/2)} - \frac{\epsilon}{2} \delta$ ▷ half-step velocity

end for

return $f(y^{(L)})$

⁸Another possible split that has some nice properties in this context is $K = \langle \rho, \rho \rangle_{g^{-1}}/2 - \log(q/\text{vol}_g)$, the Hamiltonian of the reference distribution q , and $V = \log(p/q)$. The first flow can be easily solved analytically if q is the standard normal distribution. This way, the integration error will go to zero as the Fisher divergence between q and p goes to zero.

C. Proofs

C.1. Minimization of Fisher divergence for affine transforms

Theorem C.1. *Let $x^{(i)}$ be draws from a distribution with density p and $F_{A,\mu}: \mathcal{A} \rightarrow \mathcal{T}$ with $F_{A,\mu}(y) = Ay - \mu$ a family of diffeomorphisms. Then the sample Fisher divergence*

$$\widehat{D}_F(p_{\mathcal{A}}(y; F_{A,\mu}), \mathcal{N}(0, \mathbf{I})) = \frac{1}{n} \sum_i \|y^{(i)} + \beta^{(i)}\|^2$$

is minimal if

$$M \operatorname{cov}(x^{(i)}) M = \operatorname{cov}(\alpha^{(i)}), \quad \mu = \bar{x} + M\bar{\alpha},$$

where $M = (AA^\top)^{-1}$ and

$$y^{(i)} = F^{-1}(x^{(i)}) = A^{-1}(x^{(i)} - \mu) \quad (13)$$

$$\beta^{(i)} = J_F^\top(y^{(i)}) \alpha^{(i)} + \frac{\partial}{\partial y} \log |\det J_F(y^{(i)})| = A^\top \alpha^{(i)}. \quad (14)$$

Proof. Let $X = [x^{(1)}, \dots, x^{(n)}] \in \mathbb{R}^{d \times n}$ and $S = [\alpha^{(1)}, \dots, \alpha^{(n)}]$. Let $\mathbf{e} = (1, \dots, 1)^\top \in \mathbb{R}^n$, then

$$D_F = \frac{1}{n} \|A^\top S + A^{-1}(X - \mu \mathbf{e}^\top)\|_F^2, \quad (15)$$

where $\|\cdot\|_F$ is the Frobenius norm.

Optimize with respect to μ . We get

$$d_\mu D_F \propto \operatorname{tr}\left((A^\top S + A^{-1}(X - \mu \mathbf{e}^\top))^\top d_\mu (A^\top S + A^{-1}(X - \mu \mathbf{e}^\top))\right) \quad (16)$$

$$= \operatorname{tr}\left(-(S^\top A + (X^\top - \mathbf{e} \mu^\top) A^{-\top}) A^{-1} d\mu \mathbf{e}^\top\right) \quad (17)$$

$$= \operatorname{tr}((\mathbf{e}^\top \mathbf{e} \mu^\top M - \mathbf{e}^\top S^\top - \mathbf{e}^\top X^\top M) d\mu). \quad (18)$$

This is equal the constant zero function iff

$$(\mathbf{e}^\top \mathbf{e} \mu^\top M - \mathbf{e}^\top S^\top - \mathbf{e}^\top X^\top M) = 0 \quad (19)$$

or

$$\mu = \frac{1}{n} (X \mathbf{e} + M^{-1} S \mathbf{e}) = \bar{x} + M^{-1} \bar{\alpha}, \quad (20)$$

where \bar{x} and $\bar{\alpha}$ are the sample means of $x^{(i)}$ and $\alpha^{(i)}$ respectively.

Optimizing with respect to A . Write $\tilde{X} = X - \bar{x} \mathbf{e}^\top$ and $\tilde{S} = S - \bar{\alpha} \mathbf{e}^\top$ for the centered samples and scores. Then

$$\begin{aligned} d_A \widehat{D}_F &\propto \operatorname{tr}\left((A^\top S + A^{-1}(X - \mu \mathbf{e}^\top))^\top (dA^\top S - A^{-1} dA A^{-1}(X - \mu \mathbf{e}^\top))\right) \\ &= \operatorname{tr}\left((A^\top S + A^{-1}(\tilde{X} - M^{-1} \bar{\alpha} \mathbf{e}^\top)) S^\top dA\right) \\ &\quad + \operatorname{tr}\left(A^{-1}(M^{-1} \bar{\alpha} \mathbf{e}^\top - \tilde{X}) (A^\top \alpha + A^{-1}(\tilde{X} - M \bar{\alpha} \mathbf{e}^\top))^\top A^{-1} dA\right). \end{aligned}$$

Setting $d\widehat{D}_F = 0$ for all dA yields the matrix equation

$$0 = (A^\top S + A^{-1}(\tilde{X} - M^{-1} \bar{\alpha} \mathbf{e}^\top)) S^\top + A^{-1}(M^{-1} \bar{\alpha} \mathbf{e}^\top - \tilde{X}) (A^\top S + A^{-1}(\tilde{X} - M^{-1} \bar{\alpha} \mathbf{e}^\top))^\top A^{-1}. \quad (21)$$

Using $\mathbf{e}^\top \tilde{X}^\top = \mathbf{e}^\top \tilde{S}^\top = 0$ and rearranging gives

$$0 = A^\top \tilde{S} \tilde{S}^\top + A^{-1} \tilde{X} S^\top - A^{-1} \tilde{X} \tilde{S}^\top - A^{-1} \tilde{X} \tilde{X}^\top M,$$

which simplifies to the condition

$$\tilde{S} \tilde{S}^\top = M \tilde{X} \tilde{X}^\top M$$

□

C.2. Dependence on AA^\top

Theorem C.2. *Let*

$$D_F[p_\Phi \parallel q] = \frac{1}{N} \sum_{i=1}^N \|A^\top \alpha_i + A^{-1}(x_i - \mu)\|^2.$$

Then $D_F[p_\Phi \parallel q]$ depends only on the symmetric matrix AA^\top .

Proof. Expanding the squared norm gives

$$\begin{aligned} \|A^\top \alpha_i + A^{-1}(x_i - \mu)\|^2 &= \left(A^\top \alpha_i + A^{-1}(x_i - \mu)\right)^\top \left(A^\top \alpha_i + A^{-1}(x_i - \mu)\right) \\ &= \alpha_i^\top AA^\top \alpha_i + 2\alpha_i^\top AA^{-1}(x_i - \mu) + (x_i - \mu)^\top (A^{-1})^\top A^{-1}(x_i - \mu) \end{aligned}$$

Note that $AA^{-1} = I_n$ and $(A^{-1})^\top A^{-1} = (AA^\top)^{-1}$. Therefore the expression depends on A only through the value of AA^\top . \square

C.3. Minimization of KL divergence for affine transforms

Theorem C.3. *Let $x^{(i)}$ be draws from the distribution with density $p_{\mathcal{T}}$, and let $F_{\mu,A}: \mathcal{A} \rightarrow \mathcal{T}$ be the affine transformations $F_{\mu,A}(x) = Ax + \mu$. Let $p_{\mathcal{A}}$ be the density of the distribution of $p_{\mathcal{T}}$ pulled back to \mathcal{A} .*

Then

$$\arg \min \widehat{D}_{\text{KL}}(p_{\mathcal{A}}, \mathcal{N}(0, I)) = (\bar{x}, \text{cov}(x^{(i)})),$$

where $\bar{x} = \frac{1}{n} \sum x^{(i)}$ and $\text{cov}(x^{(i)})$ is the maximum likelihood covariance estimate.

Proof. Because the KL divergence is parametrization independent, we get

$$\widehat{D}_{\text{KL}}(p_{\mathcal{A}}, \mathcal{N}(0, I)) = \widehat{D}_{\text{KL}}(p_{\mathcal{T}}, \mathcal{N}(\mu, \Sigma)),$$

where $\Sigma = AA^\top$.

$$\widehat{D}_{\text{KL}}(p_{\mathcal{T}}, \mathcal{N}(\mu, \Sigma)) = \sum_{i=1}^n \log p(x^{(i)}) + \frac{1}{2} \log \det \Sigma + \frac{1}{2} (x^{(i)} - \mu)^\top \Sigma^{-1} (x^{(i)} - \mu)$$

Minimize with respect to μ .

$$d_\mu \widehat{D}_{\text{KL}}(p_{\mathcal{T}}, \mathcal{N}(\mu, \Sigma)) = \sum_{i=1}^n (x^{(i)} - \mu)^\top \Sigma^{-1} d\mu$$

is constant zero if

$$\sum (x^{(i)} - \mu)^\top \Sigma^{-1} = 0,$$

or

$$\mu = \frac{1}{n} \sum x^{(i)} = \bar{x}.$$

Minimize with respect to Σ .

We compute the differential of the KL divergence with respect to Σ :

$$d_\Sigma \widehat{D}_{\text{KL}}(p_{\mathcal{T}}, \mathcal{N}(\mu, \Sigma)) = \frac{1}{2} \sum_{i=1}^n \text{tr}(\Sigma^{-1} d\Sigma) - (x^{(i)} - \mu)^\top \Sigma^{-1} d\Sigma \Sigma^{-1} (x^{(i)} - \mu).$$

Setting $\tilde{x}^{(i)} = x^{(i)} - \mu = x^{(i)} - \bar{x}$, and using the cyclic trace property, we get

$$d_\Sigma \widehat{D}_{\text{KL}}(p_{\mathcal{T}}, \mathcal{N}(\mu, \Sigma)) = \frac{1}{2} \sum \text{tr} \left((\Sigma^{-1} - \Sigma^{-1} \tilde{x}^{(i)} (\tilde{x}^{(i)})^\top \Sigma^{-1}) d\Sigma \right).$$

This is constant zero if

$$\sum \Sigma^{-1} - \Sigma^{-1} \tilde{x}^{(i)} (\tilde{x}^{(i)})^\top \Sigma^{-1} = 0,$$

or if

$$\Sigma = \frac{1}{n} \sum_i \tilde{x}^{(i)} (\tilde{x}^{(i)})^\top = \text{cov}(x^{(i)})$$

\square

C.4. Exact recovery for multivariate normal distributions

Let $X, S \in \mathbb{R}^{d \times k}$ be the matrix of centered draws and corresponding scores of $\mathcal{N}(\mu, \Sigma)$. Let A be a solution to $AA^\top SS^\top AA^\top = CC^\top$. We will show that $AA^\top = \Sigma$ restricted to the column space of C or that $Mv = \Sigma v$ for all $v \in \text{col}(C)$.

Proof. A little algebra shows that $S = -\Sigma^{-1}C$. Set $N = \Sigma^{-1/2}AA^\top\Sigma^{-1/2}$ and $P = \Sigma^{-1/2}CC^\top\Sigma^{-1/2}$. Then our equation becomes

$$NPN = P.$$

Let

$$P = UD'U^\top = \begin{bmatrix} Q & Q_\perp \end{bmatrix} \begin{bmatrix} D & 0 \\ 0 & 0 \end{bmatrix} \begin{bmatrix} Q^\top \\ Q_\perp^\top \end{bmatrix}$$

be the singular value decomposition of P , such that $D \succ 0$, and write

$$UNU^\top = \begin{bmatrix} A & B \\ B^\top & E \end{bmatrix}.$$

We get

$$\begin{bmatrix} A & B \\ B^\top & E \end{bmatrix} \begin{bmatrix} D & 0 \\ 0 & 0 \end{bmatrix} \begin{bmatrix} A & B \\ B^\top & E \end{bmatrix} = \begin{bmatrix} ADA & ADB \\ B^\top DA & B^\top DB \end{bmatrix} = \begin{bmatrix} D & 0 \\ 0 & 0 \end{bmatrix}.$$

The lower right block gives us $B^\top DB = 0$, and because $D \succ 0$, this implies $B = 0$. The upper left block gives us $ADA = D$. But because $D \succ 0$ and $A \succeq 0$ this implies $A = I$.

Therefore

$$UNU^\top = \begin{bmatrix} I & 0 \\ 0 & E \end{bmatrix},$$

so N acts like the identity on $\text{col}(Q) = \text{col}(P)$.

Now, let $v \in \text{col}(C)$. Since $\text{col}(P) = \text{col}(\Sigma^{-1/2}C)$, we have $\Sigma^{-1/2}v \in \text{col}(P)$. Therefore, $N\Sigma^{-1/2}v = \Sigma^{-1/2}v$. Multiplying by $\Sigma^{1/2}$ gives the desired $AA^\top v = \Sigma v$. \square

C.5. Minimum of low-rank transformation

Let $C \in \mathbb{R}^{d \times k}$ be the matrix of centered draws, $S \in \mathbb{R}^{d \times k}$ be the matrix of centered scores, and $M \in \mathbb{R}^{d \times d}$ be the symmetric, positive-definite mass matrix.

Given a regularization parameter $\gamma \in \mathbb{R}^+$, the transformation is optimal if it satisfies the condition:

$$M(\gamma I + CC^\top)M = \gamma I + SS^\top$$

We define an orthogonal matrix $Q = [Q_{2k}, Q_r]$ such that $QQ^\top = I$, where $Q_{2k} \in \mathbb{R}^{d \times 2k}$ spans the joint column space of C and S . By construction, the orthogonal complement Q_r satisfies

$$Q_r^\top C = 0 \quad \text{and} \quad Q_r^\top S = 0$$

To find the optimal M , we project the optimality condition onto the basis Q by pre-multiplying by Q^\top and post-multiplying by Q :

$$Q^\top M(\gamma I + CC^\top)MQ = Q^\top(\gamma I + SS^\top)Q$$

Because $QQ^\top = I$, we can insert the identity between the terms on the left side:

$$(Q^\top MQ)(\gamma I + Q^\top CC^\top Q)(Q^\top MQ) = \gamma I + Q^\top SS^\top Q$$

Let $\tilde{M} = Q^\top MQ$ be the mass matrix in the projected space. We partition \tilde{M} into blocks corresponding to Q_{2k} and Q_r :

$$\tilde{M} = \begin{bmatrix} M_{2k} & M_{12} \\ M_{12}^\top & M_r \end{bmatrix}$$

Because Q_r is orthogonal to C and S , the projected covariance matrices are strictly block-diagonal. Letting $C_{2k} = Q_{2k}^\top C$ and $S_{2k} = Q_{2k}^\top S$, we have:

$$\begin{bmatrix} M_{2k} & M_{12} \\ M_{12}^\top & M_r \end{bmatrix} \begin{bmatrix} \gamma I + C_{2k} C_{2k}^\top & 0 \\ 0 & \gamma I \end{bmatrix} \begin{bmatrix} M_{2k} & M_{12} \\ M_{12}^\top & M_r \end{bmatrix} = \begin{bmatrix} \gamma I + S_{2k} S_{2k}^\top & 0 \\ 0 & \gamma I \end{bmatrix}$$

For brevity, let $D_C = \gamma I + C_{2k} C_{2k}^\top$ and $D_S = \gamma I + S_{2k} S_{2k}^\top$. Expanding the left side via block-matrix multiplication yields:

$$\begin{bmatrix} M_{2k} D_C M_{2k} + \gamma M_{12} M_{12}^\top & M_{2k} D_C M_{12} + \gamma M_{12} M_r \\ M_{12}^\top D_C M_{2k} + \gamma M_r M_{12}^\top & M_{12}^\top D_C M_{12} + \gamma M_r^2 \end{bmatrix} = \begin{bmatrix} D_S & 0 \\ 0 & \gamma I \end{bmatrix}$$

Equating the corresponding blocks gives us a system of equations. From the top-right block, we have:

$$M_{2k} D_C M_{12} + \gamma M_{12} M_r = 0$$

Because M is symmetric and positive-definite, its principal submatrices M_{2k} and M_r are also symmetric and positive-definite. Furthermore, D_C is strictly positive-definite ($\gamma > 0$). Therefore, the product $M_{2k} D_C$ has strictly positive eigenvalues. The equation above is a homogeneous continuous Sylvester equation of the form $AX + XB = 0$, where $A = M_{2k} D_C$, $X = M_{12}$, and $B = \gamma M_r$. Because A and B both have strictly positive eigenvalues, their spectra are disjoint, meaning the unique solution to this Sylvester equation is the zero matrix:

$$M_{12} = 0$$

Substituting $M_{12} = 0$ into the bottom-right block equation yields:

$$\gamma M_r^2 = \gamma I \implies M_r^2 = I$$

Since M_r must be positive-definite, the unique solution is $M_r = I$. This proves that the optimal transformation acts purely as the identity on the orthogonal complement Q_r . Finally, substituting $M_{12} = 0$ into the top-left block gives the reduced optimality condition:

$$M_{2k} (\gamma I + C_{2k} C_{2k}^\top) M_{2k} = \gamma I + S_{2k} S_{2k}^\top$$

Solving the $O(d^3)$ dense optimality condition is mathematically equivalent to solving the exact same problem in the $O(k^3)$ projected subspace and padding the remaining dimensions with the identity matrix.

C.6. Minimum of diagonal transformation

Proof. Let $y = D^{-1}(x - \mu)$ be the affine transformation where $D = \text{diag}(\sigma)$. The empirical Fisher divergence between the transformed distribution and the standard normal $\mathcal{N}(0, I)$ is

$$\widehat{D}(\mu, D) = \frac{1}{n} \sum_{i=1}^n \|D\alpha_i + D^{-1}(x_i - \mu)\|^2.$$

Setting the gradient with respect to the shift μ to zero yields

$$\nabla_{\mu} \widehat{D} = -2D^{-1} (D\bar{\alpha} + D^{-1}\bar{x} - D^{-1}\mu) = 0 \implies \mu^* = \bar{x} + D^2\bar{\alpha}.$$

Because $D^2 = \text{diag}(\sigma^2)$, this is equivalent to $\mu^* = \bar{x} + \sigma^{2*} \odot \bar{\alpha}$. Substituting μ^* into the objective centers the draws and scores, $\tilde{x}_i = x_i - \bar{x}$ and $\tilde{\alpha}_i = \alpha_i - \bar{\alpha}$, decoupling the objective across the d dimensions. For each dimension j , letting $v_j = \sigma_j^2$, we minimize the quantity

$$v_j \text{var}(\alpha_j) + v_j^{-1} \text{var}(x_j) + 2\text{cov}(x_j, \alpha_j).$$

Setting the derivative with respect to v_j to zero gives

$$\text{var}(\alpha_j) - v_j^{-2} \text{var}(x_j) = 0 \implies v_j = \sqrt{\frac{\text{var}(x_j)}{\text{var}(\alpha_j)}}.$$

The affine-invariant geometric mean of two positive scalars is $a \# b = \sqrt{ab}$. Recognizing that the marginal variances are exactly the diagonals of the respective empirical covariance matrices, rewriting the element-wise optimum v_j in vector form directly yields

$$\sigma^{2*} = \text{diag}^{-1}(\text{cov}(x)) \# \left(\text{diag}^{-1}(\text{cov}(\alpha)) \right)^{-1}.$$

□

D. Adaptation online mean and variance algorithm

D.1. Welford’s algorithm

Efficient, numerically stable, single-pass estimates of the sample mean and (unbiased) sample variance via Welford’s algorithm.

Algorithm 4 WELFORD-UPDATE

Require: n : iteration, \bar{x} : running mean, x : new draw, M_2 : running sum sq. diff.

$$n \leftarrow n + 1$$

$$\delta \leftarrow x - \bar{x}$$

$$\bar{x} \leftarrow \bar{x} + \delta/n$$

$$M_2 \leftarrow M_2 + \delta \cdot (x - \bar{x})$$

return $(\bar{x}, M_2/(n - 1))$ ▷ Mean and unbiased variance

Let \bar{x}_n be the mean after n observations and $M_{2,n}$ the corresponding accumulated sum of squared deviations. When x_{n+1} arrives,

$$\bar{x}_{n+1} = \bar{x}_n + \frac{x_{n+1} - \bar{x}_n}{n + 1},$$

$$M_{2,n+1} = M_{2,n} + (x_{n+1} - \bar{x}_n)(x_{n+1} - \bar{x}_{n+1}).$$

D.2. Foreground-background modification

The removal of old draws from the Welford online estimator of draw and gradient variances is done by maintaining two parallel estimates, a “foreground” and “background”, which are stagnated to preserve the estimate when old draws are wiped. The foreground estimate is what the sampler reads from at every iteration. The background estimator, while using the same update logic, maintains a fresher estimate based on a shorter window of recent draws, and periodically hands off its fresher estimate to the foreground before resetting. The foreground estimator then builds on this estimate until being replaced by a new one from the background. A diagram of this scheme is shown in Figure 4.

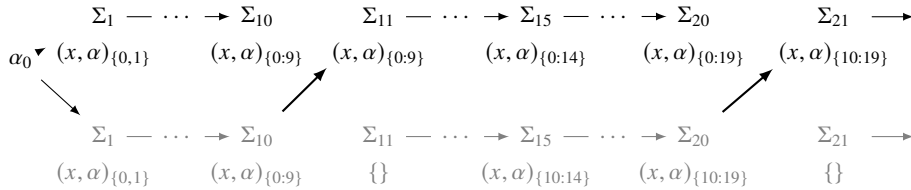


Figure 4: Example mass matrix adaptation scheme with background (below) and foreground (above) covariance estimators, with a switch/flush frequency of 10 draws. Σ_i represents the covariance estimate used to sample draw $n + 1$. Labels beneath them indicate the indices of the draw-gradient pairs on which that estimate is based. The transformation used for the Hamiltonian at each iteration is informed by the estimate stored in the foreground’s state.

E. posteriordb evaluation details

Exceptionally slow-sampling models in posteriordb that we excluded from our analysis are

ecdc0401-covid19imperial-v2,
 ecdc0401-covid19imperial-v3,
 ecdc0501-covid19imperial-v2,
 ecdc0501-covid19imperial-v3,
 election88-election88-full,

hmm-gaussian-simulated-hmm-gaussian,
iohmm-reg-simulated-iohmm-reg,
mnist-nn-rbm1bJ100,
mnist-100-nn-rbm1bJ10,
prideprejudice-chapter-ldaK5,
prideprejudice-paragraph-ldaK5

The models which did not converge for any sampler/configuration are:

GLMM-Poisson-data-GLMM-Poisson-model,
eight-schools-eight-schools-centered,
gp-pois-regr-gp-pois-regr,
low-dim-gauss-mix-collapse-low-dim-gauss-mix-collapse,
mcycle-gp-accel-gp,
mcycle-splines-accel-splines,
normal-2-normal-mixture,
normal-5-normal-mixture-k,
one-comp-mm-elim-abs-one-comp-mm-elim-abs,
ovarian-logistic-regression-rhs,
pilots-pilots,
prostate-logistic-regression-rhs,
radon-mn-radon-hierarchical-intercept-centered,
radon-mn-radon-variable-intercept-slope-centered,
radon-mn-radon-variable-slope-centered,
soil-carbon-soil-incubation,
surgical-data-surgical-model,
synthetic-grid-RBF-kernels-kronecker-gp,
three-docs1200-ldaK2,
three-men3-ldaK2,
uk-drivers-state-space-stochastic-level-stochastic-seasonal

The remaining models were

GLMM-data-GLMM1-model, GLM-Binomial-data-GLM-Binomial-model, GLM-Poisson-Data-GLM-Poisson-Data-GLM-Poisson-model, M0-data-M0-model, Mb-data-Mb-model, Mh-data-Mh-model, Mt-data-Mt-model, Mtbh-data-Mtbh-model, Mth-data-Mth-model, Rate-1-data-Rate-1-model, Rate-2-data-Rate-2-model, Rate-3-data-Rate-3-model, Rate-4-data-Rate-4-model, Rate-5-data-Rate-5-model, Survey-data-Survey-model, arK-arK, arma-arma11, bball-drive-event-0-hmm-drive-0, bball-drive-event-1-hmm-drive-1, bones-data-bones-model, butterfly-multi-occupancy, diamonds-diamonds, dogs-dogs, dogs-dogs-hierarchical, dogs-dogs-nonhierarchical, dugongs-data-dugongs-model, earnings-earn-height, earnings-log10earn-height, earnings-logearn-height, earnings-logearn-height-male, earnings-logearn-interaction, earnings-logearn-interaction-z, earnings-logearn-logheight-male, eight-schools-eight-schools-centered, firms-Aus-Jpn-irt-2pl-latent-reg-irt, garch-garch11, gp-pois-regr-gp-regr, hmm-example-hmm-example, hudson-lynx-hare-lotka-volterra, irt-2pl-irt-2pl, kidiq-kidscore-interaction, kidiq-kidscore-momhs, kidiq-kidscore-momhsiq, kidiq-kidscore-momi, kidiq-with-mom-work-kidscore-interaction-c, kidiq-with-mom-work-kidscore-interaction-z, kidiq-with-mom-work-kidscore-mom-work, kilpisjarvi-mod-kilpisjarvi, loss-curves-losscurve-sislob, low-dim-gauss-mix-low-dim-gauss-mix-collapse, lsat-data-lsat-model, mesquite-logmesquite, mesquite-logmesquite-logva, mesquite-logmesquite-logvas, mesquite-logmesquite-logvash, mesquite-logmesquite-logvolum, mesquite-mesquite, nes1972-nes, nes1976-nes, nes1980-nes, nes1984-nes, nes1988-nes, nes1992-nes, nes1996-nes, nes2000-nes, nes-logit-data-nes-logit-model, radon-all-radon-county-intercept, radon-all-radon-hierarchical-intercept-centered, radon-all-radon-hierarchical-intercept-noncentered, radon-all-radon-partially-pooled-centered, radon-all-radon-partially-pooled-noncentered, radon-all-radon-pooled, radon-all-radon-variable-intercept-slope-centered

radon-all-radon-variable-intercept-noncentered, radon-all-radon-variable-intercept-slope
radon-all-radon-variable-intercept-slope-noncentered, radon-all-radon-variable-slope-cen
radon-all-radon-variable-slope-noncentered, radon-mn-radon-county-intercept,
radon-mn-radon-hierarchical-intercept-noncentered, radon-mn-radon-partially-pooled-cen
radon-mn-radon-partially-pooled-noncentered, radon-mn-radon-pooled, radon-mn-radon-vari
radon-mn-radon-variable-intercept-noncentered, radon-mn-radon-variable-intercept-slope-n
radon-mn-radon-variable-slope-noncentered, radon-mod-radon-county, rats-data-rats-model,
rstan-downloads-prophet, sat-hier-2pl, sblrc-blr, sblri-blr, science-irt-grsm-latent-reg
seeds-data-seeds-centered-model, seeds-data-seeds-model, seeds-data-seeds-stanified-mode
sesame-data-sesame-one-pred-a, sir-sir, state-wide-presidential-votes-hierarchical-gp,
three-men1-ldaK2, three-men2-ldaK2, timssAusTwn-irt-gpcm-latent-reg-irt,
traffic-accident-nyc-bym2-offset-only, wells-data-wells-daae-c-model, wells-data-wells-d
wells-data-wells-dae-inter-model, wells-data-wells-dae-model, wells-data-wells-dist,
wells-data-wells-dist100-model, wells-data-wells-dist100ars-model, wells-data-wells-inte
wells-data-wells-interaction-model

Details and code for these models can be found [here](#). Some other interesting results from the posteriordb evaluation are found in [Figure 5](#).

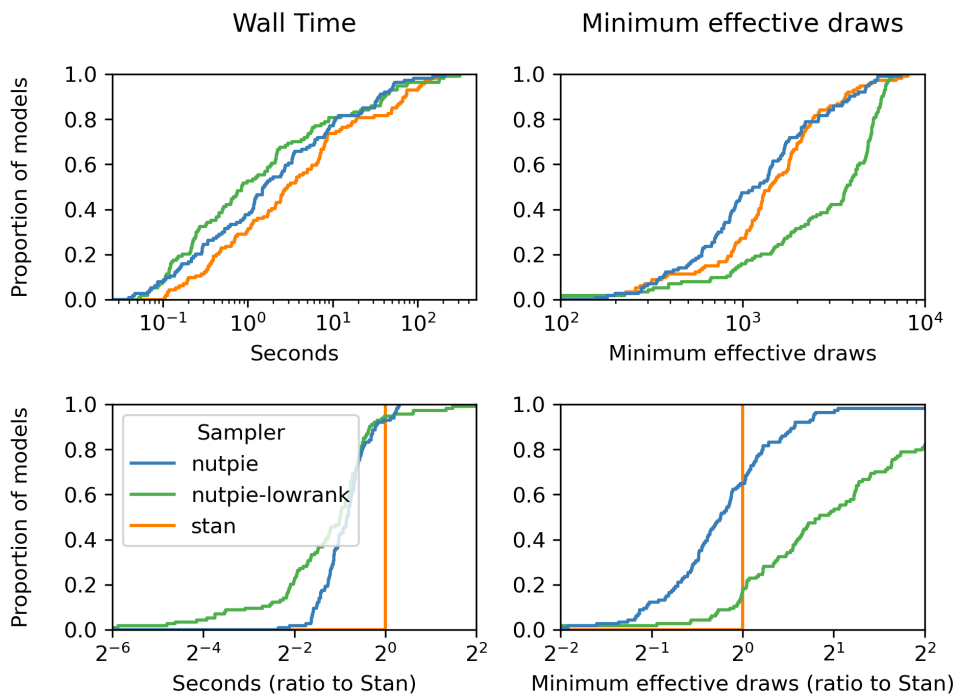


Figure 5: Cumulative distribution plots for target densities in posteriordb. Each line represents a different sampler, nutpie (blue), Stan (orange), and nutpie low-rank (green) run for 1000 warmup iterations and 1000 posterior draws. The top row of plots show the raw diagnostic, while the bottom show the ratio of the diagnostic to Stan's. In the bottom left plot, the points to the right of 1 represent a small fraction of models for which Stan's default outperforms the other options in wall time. Interestingly, for a sizable chunk models, nutpie lags behind Stan in minimum effective draws. However, this is more than made up for in the reduction in the number of required gradient evaluations.

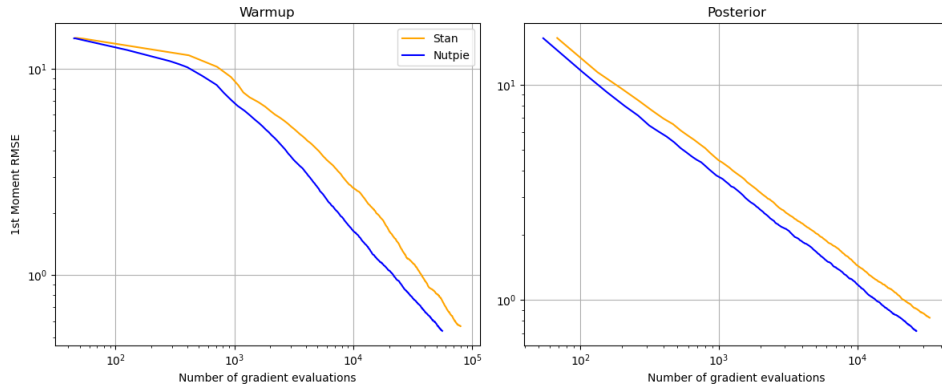


Figure 6: Average cumulative root mean squared error (RMSE) by gradient evaluations across 100 chains run for 1000 warmup draws and 500 posterior draws from a 100-D multivariate normal with a randomly generated $\Sigma = D^{1/2}U \text{diag}(\lambda^2)U^T D^{1/2}$, $U \sim \text{Uniform}(O(200))$, $\lambda_i \sim \text{exp}(2)$, $D_i \sim \text{lognormal}(0, 1)$. This procedure for generating Σ produced an eigenspectrum with a maximum eigenvalue around 20 and most fewer than 1, leading to a high condition number κ' of 68. Diagonal nutpie (blue) converged faster on average than Stan (red) in both warmup and stationary regimes, achieving a lower 1st moment RMSE in warmup with about 25,000 fewer gradient evaluations.

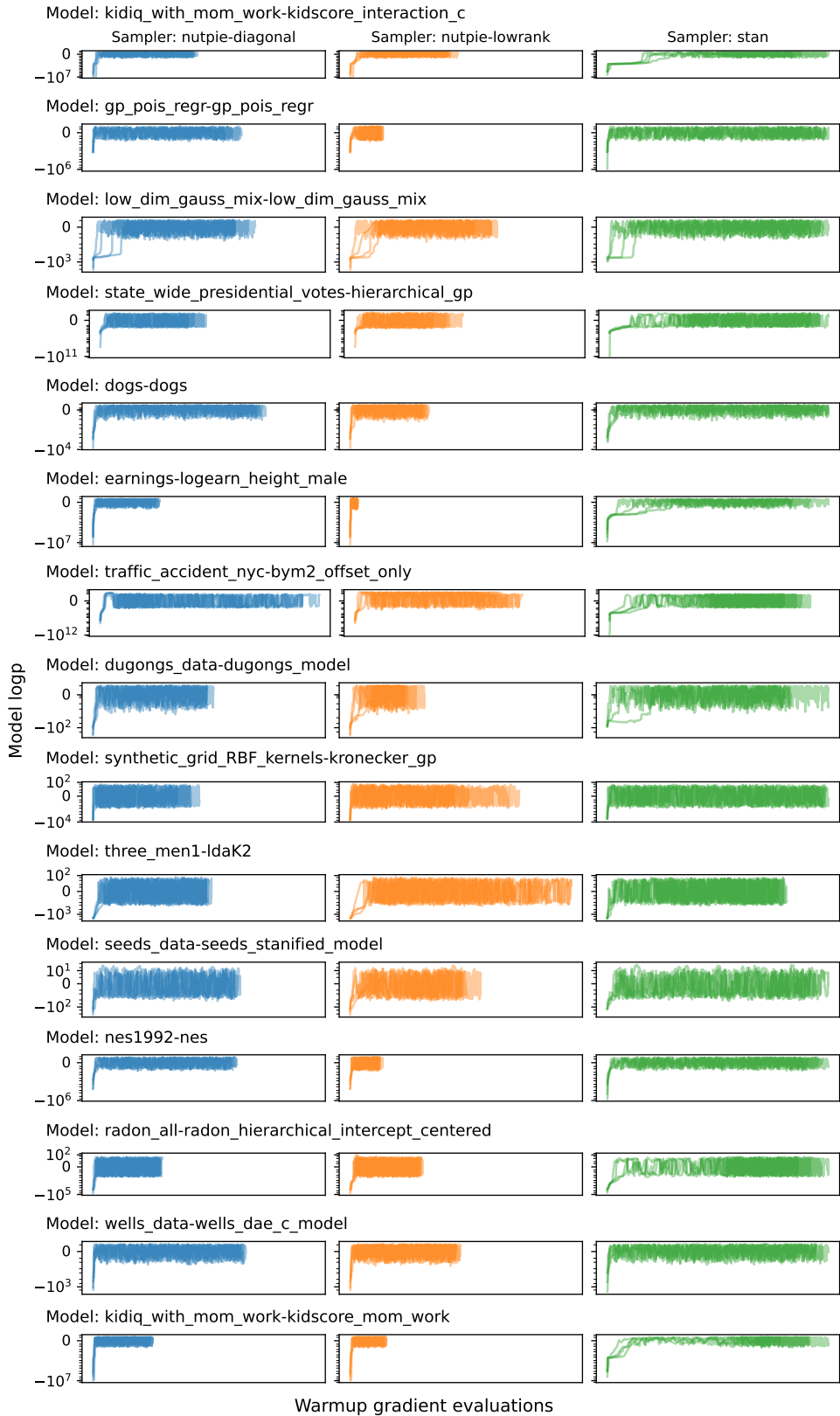


Figure 7: Trace-plots like fig. 3 of 15 randomly selected models from `posterior.db`.